OPEN EUROPEAN JOURNAL ON VARIABLE STARS
https://oejv.physics.muni.cz
October 2024 DOI: 10.5817/OEJV2024-0254 ISSN 1801–5964

NATURE AND PERIOD BEHAVIOR OF DY PEG

Berthold, Thomas[1,2]

1) Sternwarte Hartha, Töpelstr. 49, 04746 Hartha, Germany, agv@sternwarte-hartha.de
2) BAV - Bundesdeutsche Arbeitsgemeinschaft für Veränderliche Sterne, Munsterdamm 90, 12169 Berlin, Germany

Abstract: DY Peg is probably the best observed SX Phe star ever. It is one of this type's not very numerous galactic field stars. This paper uses newly gathered observations from the decade after the last published work and presents at first an extended revision of the fundamental period behavior. It turns out that a model comprising sudden period changes followed by sections with constant period length describes the way the (O-C) values behave better than the assumption of a constant amount of change, with or without a superposition with light-time effects due to an orbiting companion. Following this, a frequency analysis reveals that the star pulsates in fundamental and first overtone radial modes and shows evidence for additional non-radial oscillations. Finally, the binary and evolutionary status of DY Peg is evaluated.

1 Introduction

DY Peg (GSC 01712-01253, 2MASS J23085118+1712560) has been discovered to be a short-periodic variable by Morgenroth (1934). Shortly afterwards, Soloviev (1934) has disclosed its nature as a very short-periodic RR Lyr type star. Subsequently, it was classified as a dwarf cepheid or Delta Scuti star. It was not until 1982, when Coates, Halprin&Thompson (1982) discovered that the overtone pulsations of DY Peg exhibited striking similarities to those of SX Phe, that this classification was established. Due to its outstandingly fast light changes, the star has attracted intense attention. Monographic papers sum up the state of knowledge at the time of publication. Quigley & Africano (1979), Mahdy & Szeidl (1980), Hintz et al. (2004), Fu et al. (2009), Li & Quian (2010) and Xue & Niu (2020) stand for that. Despite a large amount of data available, there has been no conclusive proof of the reason for the observed period behavior.

An attempt is made to clarify the situation with new measurements from the last ten years and data from more recent surveys (TESS and GAIA DR3).

2 O-C diagram of the fundamental period

Table 1 provides a comprehensive overview of all available period studies published to date.

All the observed times of maximum light from the past eight decades are subsequently shown in Figure 1, employing ephemerides (1), which are the same as the initial elements in Li & Quian (2010).

$$HJD_{\mathrm{Max}} = 2438276.8643 + 0.07292633 \cdot E. \quad (1)$$

OPEN EUROPEAN JOURNAL ON VARIABLE STARS
https://oejv.physics.muni.cz
October 2024 DOI: 10.5817/OEJV2024-0254 ISSN 1801–5964

Table 1: Published period studies for DY Peg. Used maximum timings and time frame

Authors	Archival	New	Total	Total time frame [JD]
Quigley & Africano	103	19	122	2430976 - 2443353
Mahdy & Szeidl	90	10	100	2429193 - 2444113
Hintz et al.	208	69	277	2429193 - 2452903
Fu et al.	277	121	398	2429193 - 2454779
Li & Quian	410	2	412	2432751 - 2454828
Xue & Niu	412	277	689	2432751 - 2458781
This Paper	689	145	834	2429193 - 2460262

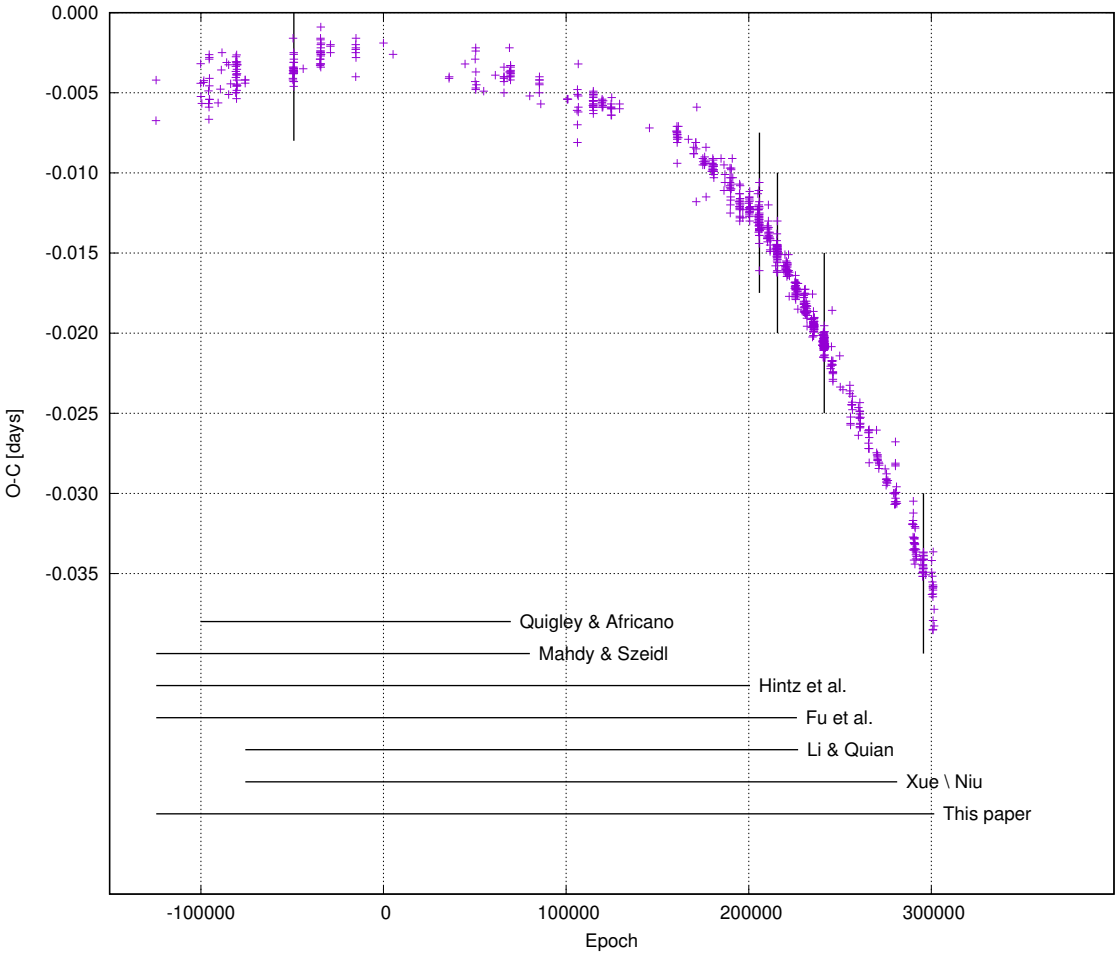

Figure 1: O-C diagram of DY Peg corresponding to ephemeris (1). Horizontal lines visualize the observational time base of the data sets used in the studies published so far. Vertical lines mark the times of frequency studies made by Kozar (1980), Fu et al. (2009)(2), Xue & Niu (2020) and in this paper (from left to right).

October 2024 DOI: 10.5817/OEJV2024-0254 ISSN 1801–5964

The dominant structure in Figure 1 is a persistent shortening of the period lasting at least eight decades. In the past, various authors have proposed several models to describe this situation.

The most straightforward approach describes such a behavior through multiple sections of constant period, with abrupt and irregular changes. Hintz et al. (2004) and Fu et al. (2009) have computed sets of linear elements for three time intervals by applying this method to their data sets.

Adding the times of maximum that are available now, it is possible to repeat the evaluations and to add a fourth interval.

Valid for Maxima from Julian Date 2429193 - 2438655 / Epochs -124556 - 5197:

$$HJD_{\mathrm{Max}} = 2438276.8624(2) + 0.072926357(3) \cdot E \qquad \sigma = 0\overset{\mathrm{d}}{.}0008 \tag{2}$$

$$\Delta P/P = -0,88 \cdot 10^{-6}$$

Valid for Maxima from Julian Date 2440895 - 2450667 / Epochs 35910 - 169912:

$$HJD_{\mathrm{Max}} = 2438276.8628(2) + 0.072926293(2) \cdot E \qquad \sigma = 0\overset{\mathrm{d}}{.}0007 \tag{3}$$

$$\Delta P/P = -2,29 \cdot 10^{-6}$$

Valid for Maxima from Julian Date 2450742 - 2458760 / Epochs 170937 - 280885:

$$HJD_{\mathrm{Max}} = 2438276.8929(4) + 0.072926125(2) \cdot E \qquad \sigma = 0\overset{\mathrm{d}}{.}0009 \tag{4}$$

$$\Delta P/P = -1,69 \cdot 10^{-6}$$

Valid for Maxima from Julian Date 2458721 - 2460262 / Epochs 280345 - 301476:

$$HJD_{\mathrm{Max}} = 2438276.9267(47) + 0.072926002(16) \cdot E \sigma = 0\overset{\mathrm{d}}{.}0009 \tag{5}$$

Sudden period changes of such a scale, i.e. in the order of $\Delta P/P = 10^{-6}$, are common for SX Phe stars (Breger & Pamyatnykh (1998). Nevertheless, the division into four sections is not definitive, e.g. one more section could easily be inserted between ephemerides (3) and (4).

These erratic period changes could be attributed to superposition effects of the various radial and non-radial pulsation modes or to temporary instabilities within a circumstellar disk, which would lead to an episodic mass transfer. However, there is no evidence of an infrared excess associated with a dust disk around DY Peg.

Alternatively a parabolic adjustment should be attempted, as it is commonly done in such cases. A solution using the least squares method provides the elements (6) with the grahic presentation in Fig. 4.

$$HJD_{\mathrm{Max}} = 2438276.8639(1) + 0.072926353(1) \cdot E - 4.48(5) \cdot 10^{-13} \cdot E^2 \qquad \sigma = 0\overset{\mathrm{d}}{.}0015 \tag{6}$$

For comparison, Table 3 presents the coefficient of the square term and the corresponding period decrease as published by the other authors. The residuals from the above parabola are given in Fig. 5.

https://oejv.physics.muni.cz
October 2024 DOI: 10.5817/OEJV2024-0254 ISSN 1801–5964

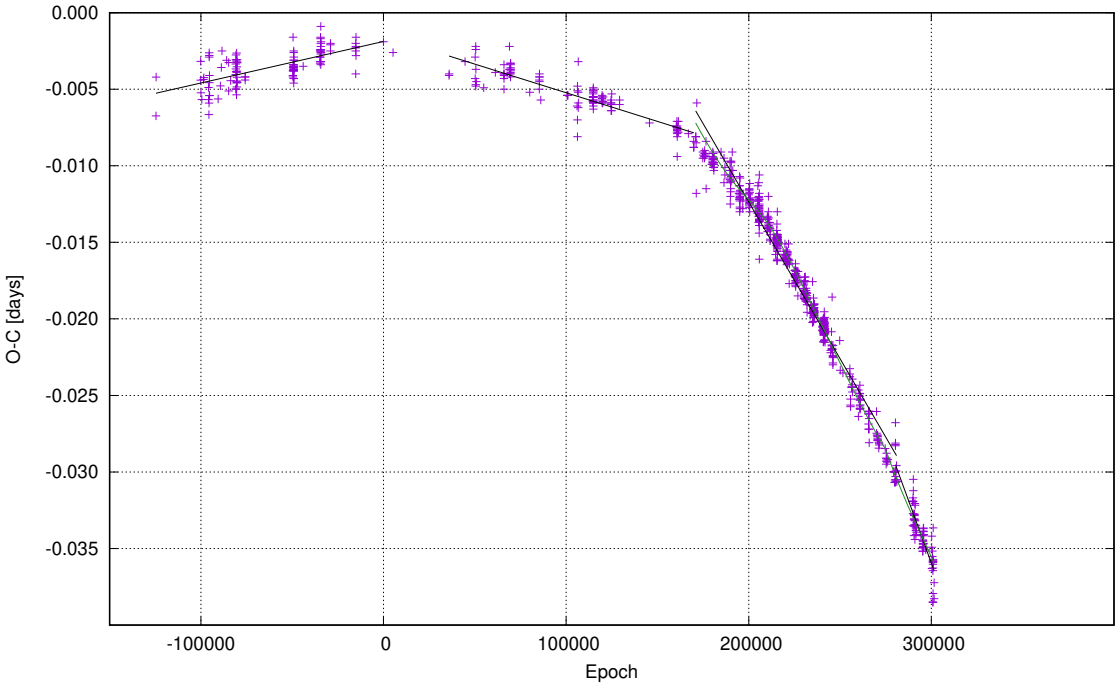

Figure 2: O-C diagram of DY Peg corresponding to the linear solutions from ephemeris (2)-(5). The superimposed LiTE fit is represented with the green line (Slight effect - difficult to discern in the graphic.)

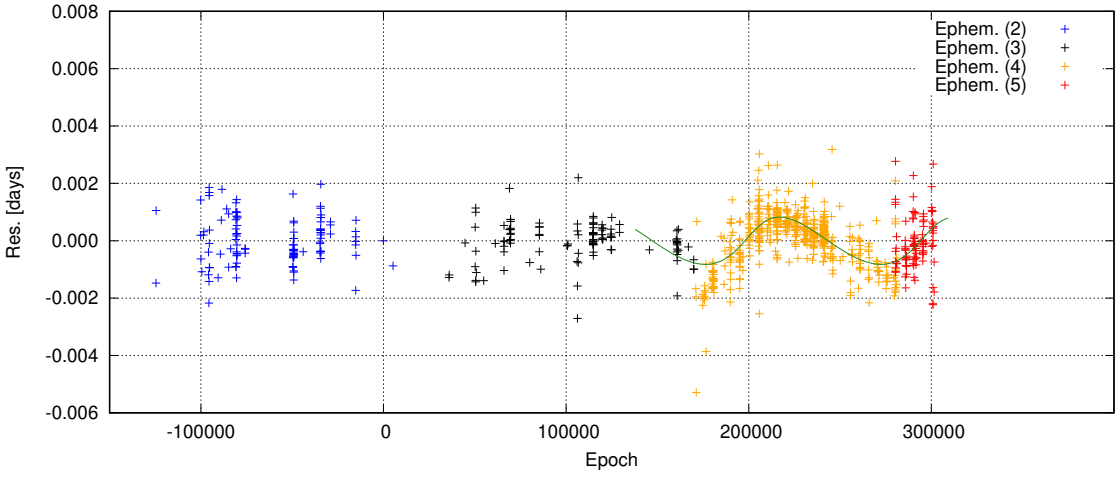

Figure 3: Residuals corresponding to the linear solution from ephemeris (2)-(5). The remaining overall standard deviation is $\sigma = 0\overset{d}{.}0009$. The green line represents the results of a Monte Carlo simulation for the contribution of the light-time effect for a star in a binary system. The application of this fit is limited to the newer observations (cycles approx. 150.000-300.000), and therefore the resulting solution is somewhat arbitrary.

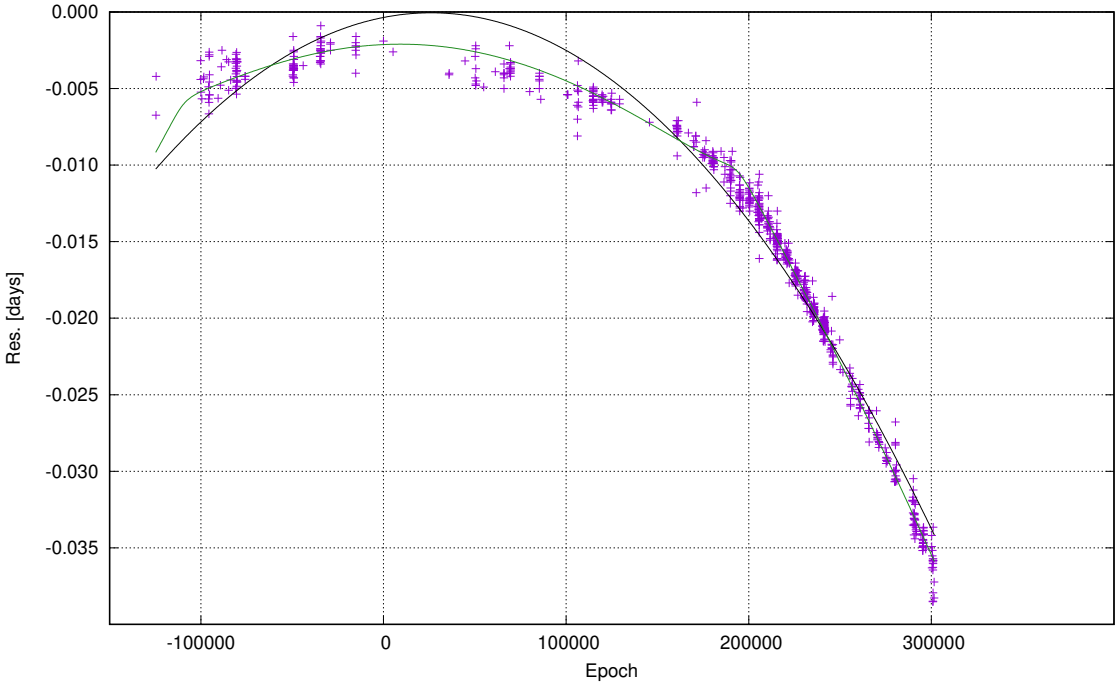

Figure 4: O-C diagram of DY Peg. The black line gives the quadratic solution from ephemeris (6). The superimposed LiTE fit is represented with the green line

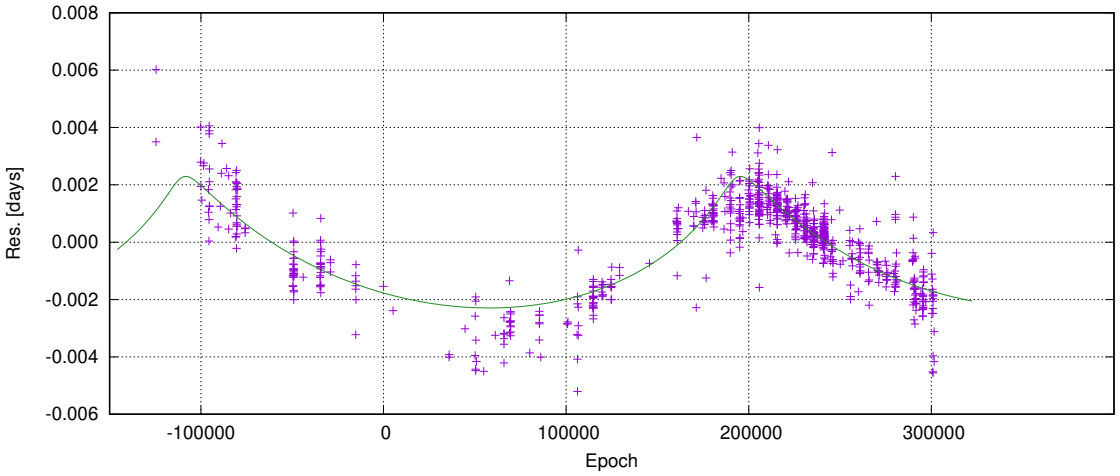

Figure 5: Residuals corresponding to the quadratic solution from ephemeris (6). The green line represents the results of a Monte Carlo simulation for the contribution of the light-time effect for a star in a binary system.

October 2024 DOI: 10.5817/OEJV2024-0254 ISSN 1801–5964

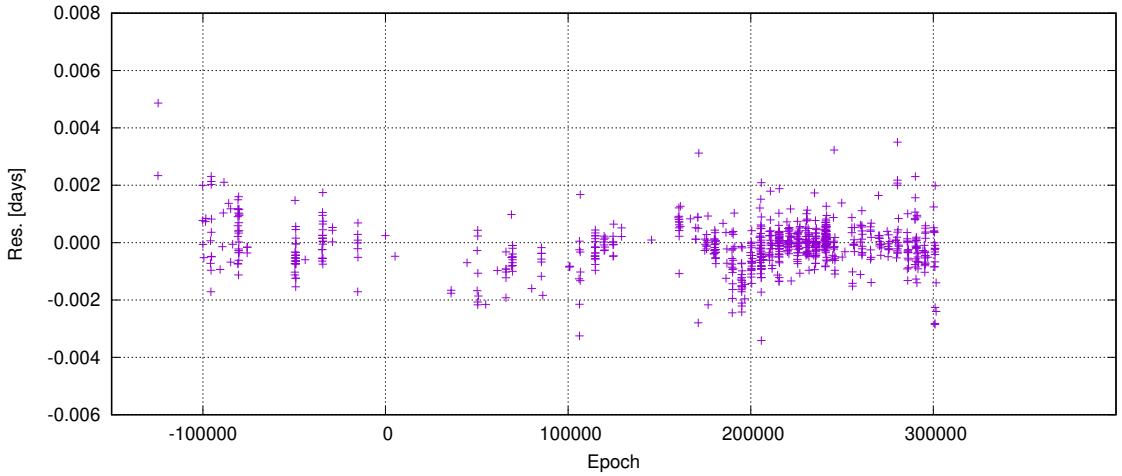

Figure 6: Remaining residuals corresponding to LiTE solution applied to ephemeris (6). The standard deviation is $\sigma = 0\overset{\mathrm{d}}{.}0008$.

Table 2: Bayesian Information Criterion for the two modes of period behavior

Mode	Ephemeris	BIC
Linear	(2) – (5)	−6.11
Quadratic	(6)	−5.61

Given the relatively equal levels of the residuals, it is not possible to decide how to describe the period change based only on the standard deviations. The Bayesian Information Criterion (BIC) may be an appropriate instrument for this objective. It offers a strategy for selecting the most suitable model from a given set of models based on the number of free parameters required to represent measurements with a specified standard deviation. The BIC is defined as

$$BIC = \frac{p \cdot \log N}{N} + \log\left(\sigma^2\right) \tag{7}$$

where p is the number of free parameters, N is the number of data points, and σ gives the standard deviation of the residuals. The results, which are listed in Table 2, indicate that a description of the behavior of DY Peg with sudden period changes followed by several constant phases is the slightly more probable hypothesis.

The data presented in Figure 5 and, to a lesser extent, in Figure 3 suggest that there may be a possibility of superimposing a periodic pattern on the quadratic as well as the linear approach.

Consequently, orbits are computed to incorporate the appropriate light-time effect (LiTE) effects to replicate the observed deviations by superimposing an underlying linear or parabolic period change with better precision. These LiTE orbit data were calculated from the residuals with Monte Carlo Simulations using the OCFit package (Gajdoš & Parimucha (2023)).

Table 3: Published values for the amount of the constant period decrease

Authors	$dP/dt = \beta$ [d/cycle]	$1/P(dP/dt)$ [a^{-1}]	Remarks
Quigley & Africano	$-4.59 \cdot 10^{-13}$	$-3.155 \cdot 10^{-8}$	
Mahdy & Szeidl	$-7.63 \cdot 10^{-13}$	$-5.237 \cdot 10^{-8}$	
Hintz et al.	$-4.37 \cdot 10^{-13}$	$-3.004 \cdot 10^{-8}$	
Fu et al.	$-5.00 \cdot 10^{-13}$	$-3.434 \cdot 10^{-8}$	LiTE
Li & Quian	$-6.59 \cdot 10^{-13}$	$-4.526 \cdot 10^{-8}$	LiTE
Xue & Niu	$-8.55 \cdot 10^{-13}$	$-5.872 \cdot 10^{-8}$	LiTE
This Paper	$-8.95 \cdot 10^{-13}$	$-6.135 \cdot 10^{-8}$	LiTE

Table 4: Binary orbit solution. Significant differences exist between the values presented in the text and the figures in Fu et al. (2009).

Authors	A [days]	$a \cdot sin(i)$ [au]	e	ω [deg]	T	P_{B} [yrs]
Fu et al. (text)	0.172	29.9	1.0	-	2454877	88.7
Fu et al. (figures)	0.00185	0.321	-	-	-	51.9
Li & Quian	0.00147(20)	0.254(34)	0.65(10)	180.7(103)	2454074(233)	42.2(15)
Xue & Niu	0.00204(3)	0.353(5)	0.244(8)	239.0(52)	2457942(159)	42.2(6)
This Paper Ephem. (6)	0.00235(13)	0.407(22)	0.76(2)	73(8)	2452358(332)	60.6(4)
This Paper Ephem. (2)-(5)	0.00085(4)	0.147(8)	0.26(9)	19(14)	2453000(276)	19.2(3)

Table 4 summarises the orbit determination results obtained from analysing the maximum times shifted by LiTE effects. There, $A = a \cdot sin(i)/c$ is the projected semi-major axis, e is the eccentricity, ω the argument of periastron, T is the time of passage through the periastron and P_{B} is the orbital period of the binary system. A view to the first line of Table 4 reveals that the numerical values presented in the text section of the paper by Fu et al. (2009) are erroneous. A reading from the figures presented in their paper yields more plausible data. These values (second line of Table 4), along with those presented by Li & Quian (2010) and Xue & Niu (2020), as well as the values derived from the ephemeris (6) in this paper, pertain to the parabolic model of the (O-C) curve and are, thus, essentially comparable. The calculated values were anticipated to tend towards stability as the time base was extended. However, this is not the case. At best, there was a rough agreement, which did not inspire confidence in this approach. The final line in Table 4 presents the calculated values for a part of the LiTE overlay of the linear period sections, provided for comparison purposes only.

Regarding determining the most suitable description for the observed period changes, please refer to subchapter 4.2.

October 2024 DOI: 10.5817/OEJV2024-0254 ISSN 1801–5964

3 Frequency analysis

The first indications for dual-mode pulsations can be found in the work of Kozar (1980), who detected the two radial modes in the observation set of Masani & Broglia (1954). His periodogram analysis according to the method of Wehlau & Leung (1964) resulted in a ratio of $f_0/f_1 = 0.7638$. Repeated frequency studies have been performed later by Fu et al. (2009) and Xue & Niu (2020) over the last 100.000 epochs as more extensive V-band data sets of DY Peg have become available. This procedure was repeated in the present study with extremely rich and accurate TESS observations. Multi-Aperture Photometry data from the TESS Quick-Look Pipeline were used. The detrended flux values were obtained from the MAST Portal (Targetname: 218046347). The Period04 software package (Lenz & Breger (2005)) was used to search for significant frequency peaks in these three studies. The results obtained with the Fourier analysis are compared in Tables 5 and 6.

Table 5: Significant frequencies with their normalized intensities obtained after stepwise pre-whitening. SNR boxwidth unknown. The time of observation is indicated by the years in brackets.

Number	Mode	Kozar (1953)		Fu (2004)			Fu (2006)		
		Freq.	Int.	Freq.	Int.	SNR	Freq.	Int.	SNR
1	f_0	13.7126	1.000	13.7127	1.000	186.3	13.7130	1.000	217.6
2	$2f_0$	27.4248	0.413	27.4254	0.344	88.8	27.4248	0.345	85.3
3	$3f_0$	41.1384	0.0157	41.1381	0.117	51.8	41.1385	0.119	40.4
4	$4f_0$	54.8464	0.073	54.8508	0.050	32.5	54.8469	0.049	22.0
5	$5f_0$	68.5560	0.028	68.5633	0.022	16.0	68.5532	0.021	9.2
6	$6f_0$	82.2831	0.017	-	-	-	-	-	-

Table 6: Significant frequencies with their normalized intensities as obtained after stepwise pre-whitening. SNR is calculated with a boxwidth of $6c/d$. The time of observation is indicated by the years in brackets.

Number	Mode	Xue et al. (2011)			This paper (2022)		
		Freq.	Int.	SNR	Freq.	Int.	SNR
1	f_0	13.7125	1.000	112.6	13.7125	1.000	841.2
2	$2f_0$	27.4251	0.342	104.2	27.4251	0.380	403.9
3	$3f_0$	41.1374	0.118	68.8	41.1375	0.140	165.5
4	$4f_0$	54.8502	0.050	45.2	54.8500	0.058	68.4
5	$5f_0$	68.5626	0.021	25.7	68.5619	0.025	29.7
6	f_1	17.7000	0.022	6.6	17.7005	0.022	22.1
7	$f_0 + f_1$	31.412	0.011	6.1	31.4130	0.014	15.2
8	$6f_0$	82.275	0.011	13.4	82.2741	0.011	13.3
9	$f_1 - f_0$	4.016	0.012	4.8	3.9883	0.011	8.9
10	f_2	18.138	0.012	6.7	18.1381	0.009	9.3
11	$2f_0 + f_1$	45.122	0.007	6.1	45.1267	0.008	9.3
12	$7f_0$	95.987	0.007	16.4	95.9885	0.007	8.0
13	$f_0 + f_2$	31.851	0.007	6.8	31.8483	0.006	6.5
14	$3f_0 + f_1$	-	-	-	58.8390	0.005	5.4
15	$2f_0 - f_1$	-	-	-	9.7232	0.005	4.1
16	$8f_0$	109.702	0.005	6.7	109.7014	0.004	4.2

All studies show the typical behavior of an SX Phe star pulsating in two radial modes f_0 and f_1. The relationship of $f_0/f_1 = 0.775$ agrees perfectly with the theoretical models for pulsations in the fundamental and first overtone radial modes (see e.g. Poretti Poretti et al. (2005)).

First detected by Xue & Niu (2020), a frequency f_2 with $f_0/f_2 = 0.7560$ is also found, although very weak, in the TESS data set. In any case, this frequency ratio indicates that f2 is a non-radial mode.

4 Model and evolutionary status

4.1 Physical Parameters

Obtaining precise values for individual stars is a quite challenging endeavor. In the past, these values were derived from dust maps for most analogous studies. However, with the advent of the GAIA survey, values have become available for certain objects. Unfortunately, both values differ considerably in the case of DY Peg. It is difficult to determine which variant is more reliable for that specific star, so it seems prudent to continue with the two values as assumed extremes. A value for the interstellar extinction can be derived from the standard dust reddening map of Schlegel, Finkbeiner & Davis (1998), queried with the NASA/IPAC dust and extinction tool, to $A_v = 0.410(28)$ mag. GAIA DR3 (Vallenari et al. (2023)) marks the opposite end of the range, with an $A_v = 0.173(17)$ mag.

Then, absolute visual magnitudes can be obtained with a GAIA DR3 distance of $d = 407(7)$ pc and the mean V magnitude of Burki & Meylan (1986) $m_v = 10.31$ mag using the relation

$$M_v = V - 5 \log d + 5 - A_v \tag{8}$$

This results in an absolute magnitude of $M_v = 1.97(22)$ mag. Taking the mean effective temperature from Burki & Meylan (1986) to $T_{\rm eff} = 7240(100)$ K, the bolometric correction is found to be 0.034(1) mag from Table 3 of Flower (1996). Thus, the absolute bolometric magnitude can be obtained to 2.00(23) mag.

Using that absolute bolometric magnitude and a value for the sun of 4.74(10) mag (somewhat problematic, see Torres (2010) Table 3 for details), a luminosity ratio can be calculated via:

$$\log(L/L_\odot) = -0.4(M_{bol} - M_{bol\odot}) \tag{9}$$

The impact of the uncertain level of the absolute brightness is evident in a considerable inaccurate luminosity value of $L = 13.1(38)L_\odot$.

The Stefan-Bolzmann law can be used to derive the radius of the star. In values of the corresponding properties of the sun, it can be expressed as

$$R/R_\odot = \sqrt{(L/L\odot)/(T/T\odot)^4} \tag{10}$$

where $T_\odot = 5772K$ according to Prša et al. (2016), and the luminosity ratio comes from Eq.9. This results in a radius of $R = 2.28(41)R_\odot$.

October 2024 DOI: 10.5817/OEJV2024-0254 ISSN 1801–5964

Several mass-luminosity relations (MLRs) are currently in use. These relations are founded upon data obtained from the components of detached eclipsing spectroscopic binaries or are derived from pulsation theory. An empirical MLR as derived by Eker et al. (2018) can provide an independent way to determine the mass of single stars. For an expected stellar mass in the range $1.05 < M/M_{\odot} \leq 2.40$, the relation is

$$\log(L) = 4.329(87) \cdot \log(M) + 0.010(19) \tag{11}$$

what leads to a stellar mass of $M = 1.79(16)M_{\odot}$.

According to the works of both Hintz et al. (2004) and Burki & Meylan (1986), a consistent value for metallicity can be set at $[Fe/H] = -0.8$. With $Z_{\odot} = 0.0134$ as the solar value (Asplund et al. (2009)) and the relation

$$Z = 10^{[Fe/H]} \cdot Z_{\odot} \tag{12}$$

it results in DY Peg having a metallicity of $Z = 0.002$. At this point, it is worth noting that a small excess of calcium, sulfur and carbon was established. Since these elements could only be produced in the later stages of the stellar evolution, they could not have come from DY Peg itself. Instead, they have to come from an evolved companion. This will be discussed in the next subchapter.

4.2 Binarity

With the above calculated stellar mass of $M_1 = 1.79M_{\odot}$ and with the values for the mass function

$$f(M) = \frac{{M_2}^3 \cdot \sin(i)^2}{(M_1 + M_2)} \tag{13}$$

from the LiTE analysis, we can determine the companion's mass as a function of the orbital inclination. Both cases are demonstrated in Figure 7. Given that the inclinations are evenly distributed, a companion of relatively low mass seems likely. This corresponds to a relatively low level of additional brightness for the system, as the absolute magnitude of DY Peg, as derived before, is incompatible with a luminous companion.

Given that the mass of an accompanying white dwarf (WD) must fall within the range of 0.2 to 1.4 solar masses, Kepler's third law can be employed to calculate the orbital period of such a system. The results for the eligible pairs are presented in Table 7.

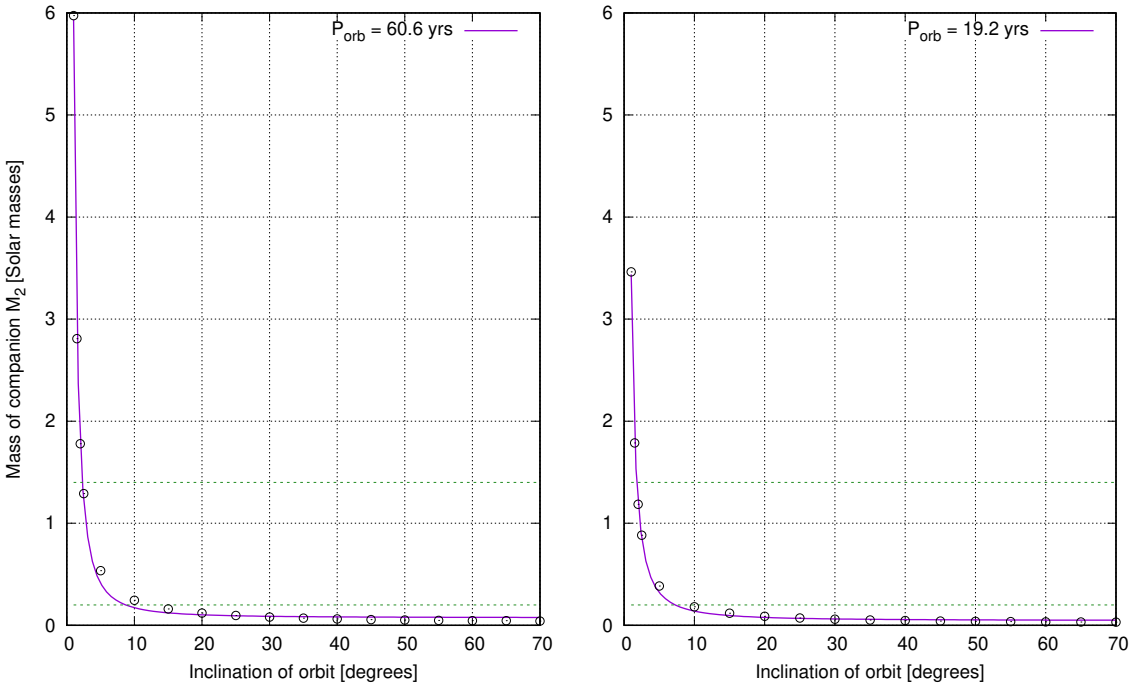

Figure 7: Mass M_2 and inclination of the orbital plane for the two LiTe solutions. The dashed green lines mark the mass limits for white dwarfs $[0.2, 1.4]M_\odot$.

As can be seen from this table, there is no instance in which the Keplerian period coincides with the LiTE orbital period. This leads to the following conclusions:

- It is not appropriate to interpret the run of (O-C) values as a LiTE superposition of linear or quadratic elements.
- Without this, the remaining residuals from a pure parabola are unsatisfactorily large in case of the quadratic solution. Furthermore, the higher BIC value indicates that the quadratic model is not the optimal choice.
- The period behavior of DY Peg should therefore better be interpreted as a sequence of sudden period changes followed by sections with constant period length. This is not surprising because such an observational pattern has been considered a typical characteristic of SX Phe stars since the work of Breger & Pamyatnykh (1998).
- Eqs. 2 - 5 describe the repetitive period decreases, which can occur independently from the general stellar evolution. Therefore, a successive shortening of the period is not required. Despite its detailed construction, the model of Xue & Niu (2020) with a mass-accreting star is no longer necessary to explain the observed period changes without contravening evolutionary models that predict an increase in the period.
- The measured excess of α-elements is quite small (Hintz et al. (2004)). If there is any contamination with these elements at all, this would, of course, require an evolved companion (probably a WD). It would, however, be in an orbit whose LiTE effects are not discernible within the limitations of the available observational data set.

October 2024 DOI: 10.5817/OEJV2024-0254 ISSN 1801–5964

Table 7: Binary data for components fitting the LiTE solution. Upper part: for ephemeris (6). Lower part: for ephemeris (4) and (5)

P_{LiTE} [yrs]	Mass Function [$m_\odot$]	Inclination [deg]	m_2 [$m_\odot$]	$m_1 + m_2$ [$m_\odot$]	a [au]	P_{Kepler} [yrs]
60.6(4)	1.8(3) $\cdot 10^{-5}$	2.5	1.29	3.08	9.34	16.25
		5.0	0.53	2.33	4.67	6.62
		10.0	0.25	2.04	2.35	2.52
19.2(3)	0.8(1) $\cdot 10^{-5}$	2.0	1.19	2.98	4.21	5.01
		2.5	0.88	2.67	3.37	3.78
		5.0	0.39	2.18	1.69	1.48
		10.0	0.18	1.97	0.85	0.55

4.3 Evolutionary State

The galactocentric position and velocities were taken from the dynamic data of the GAIA DR3 Chemical Cartography.

Table 8: Galactocentric data of DY Peg

Distance to the galactic plane	Velocity in z-direction	Total galactocentric velocity
-232(5) pc	-37(2) km/s	184(3) km/s

In light of this and the aforementioned metallicity value, it seems reasonable to conclude that DY Peg may be a member of the thick disk.

Nevertheless, its evolutionary state is not as straightforward to delineate. The usual way to identify an evolutionary track that aligns with the position of DY Peg in the Hertzsprung-Russell diagram is to estimate its age, but this is not a promising avenue for investigation. The reason for this is that DY Peg is not a typical main sequence star, but rather a blue straggler (BS), as has been already pointed out by several authors in the past, see for instance Burki & Meylan (1986) or, more generally, Cohen & Sarajedini (2012).

BS were originally found in galactic globular clusters, characterized by being bluer and brighter than the respective main sequence turn-off of the cluster. Carney et al. (2001) investigated the location of main sequence turnoffs in globular clusters with comparable metallicity and found the following relationship:

$$(B-V)_{0,\,\mathrm{turnoff}} = 0.615 + 0.209[Me/H] + 0.046[Me/H]^2 \qquad (14)$$

The data of this analysis, augmented by that of DY Peg, is presented in Figure 8. Carney et al. (2001) found that the thick-disk stellar population appears to have a very sharp cutout in $(B\text{-}V)_0$, consistent with the main-sequence turnoffs of the disk-population globular clusters 47 Tuc and M71. They concluded, therefore, that the field thick-disk stars are as old as the clusters in question. In comparing the development status of DY Peg with the BS of ω Cen, Burki & Meylan (1986) had already reached a similar conclusion. This conclusion remains valid if the absolute brightness is adjusted for the correct distance value, which was not available at the time of their study.

Given all the evidence above, it seems plausible to suggest that DY Peg may be a constituent of the thick disk, with a probable age of 10–12 Gyr.

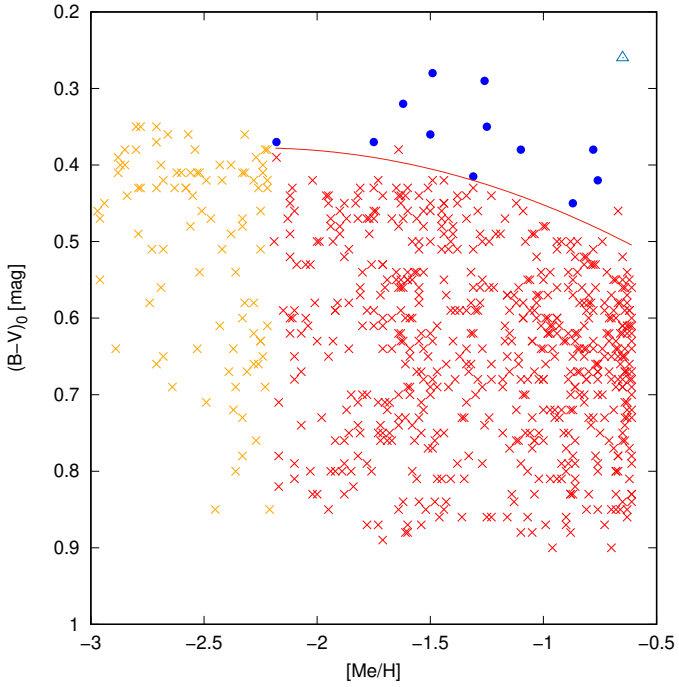

Figure 8: Photometric positioning of the galactic BS according to the methodology proposed by Carney et al. (2001), see Figure 1 therein. The position of DY Peg is marked with the open triangle. The parabola (Eq. 14) represents the main sequence turn-off loci valid for $[-2.2 < [Me/H] < -0.6]$. Field stars (crosses) and BS (filled circles) are well distinguished. For DY Peg, $(B\text{-}V)_0$=0.26 was taken from (Burki & Meylan (1986)) and [Me/H] was derived from a roughy assumed value of [α/Fe=0.2] using the equation of Salaris et al. (1993): $[Me/H] = [Fe/H] + \log(0.694 \cdot 10^{[\alpha/\mathrm{Fe}]} + 0.306)$

5 Summary

- Summarizing all aspects of this work, the light changes observed in DY Peg over a period exceeding eight decades can be described best by a sequence of abrupt period decreases, followed by periods of constant length. The rationale behind the observed repetitive period shortenings remains uncertain.

- The availability of the excellent TESS time series confirms that the star oscillates in the fundamental and the first overtone radial mode, with an observed frequency ratio of $f0/f1 = 0.775$ that is in exact accordance with the predictions of the evolutionary models. The effect of a non-radial oscillation with $f2 = 18.14d^{-1}$ could be confirmed.

- If there is an evolved companion (potentially a WD that has been formed during the evolutionary pathway of DY Peg towards a BS), it cannot be detected by LiTE effects in the (O-C)-diagram.

October 2024 DOI: 10.5817/OEJV2024-0254 ISSN 1801–5964

- The color, metallicity, and dynamic state of DY Peg within the galaxy are consistent with its classification as a member of the thick-disk population. In comparison with the turn-off positions of galactic globular clusters, an evolutionary age of 10-12 Gyr can be derived, which provides sufficient time for the formation of the BS.
- To substantiate this study's results, some additional decades of photometry and, in particular, more precise spectroscopic measurements are required. Reliable detection or exclusion of the α-elements would be beneficial in answering the question of the existence of an evolved companion. Despite the extensive and detailed research conducted so far, DY Peg remains a topic worthy of further investigation and analysis.

Acknowledgements: This research has made use of data from:

- The SIMBAD database and the VizieR catalogue access tool, operated at CDS, Strasbourg, France (Wenger et al. (2009))
- The Mikulski Archive for Space Telescopes (MAST, https://archive.stsci.edu/index.html)
- The TESS mission, obtained from the MAST data archive at the Space Telescope Science Institute (STScI)
- The European Space Agency (ESA) mission Gaia (https://www.cosmos.esa.int/gaia), processed by the Gaia Data Processing and Analysis Consortium (DPAC, https://www.cosmos.esa.int/web/gaia/dpac/consortium)
- The NASA/IPAC Infrared Science Archive, which is funded by the National Aeronautics and Space Administration and operated by the California Institute of Technology (https://irsa.ipac.caltech.edu/frontpage/)
- The AAVSO International Database contributed by observers worldwide (https://www.aavso.org)

References

Asplund, M. et al. 2009, *Annual Review of Astronomy & Astrophysics* , **47**, 481, 2009ARA&A..47..481A

Balona, L. A. & Nemec, J. M. 2012, *Monthly Notices of the Royal Astronomical Society* , **426**, 2413, 2012MNRAS.426.2413B

Breger, M. & Pamyatnykh, A. A., *Astronomy and Astrophysics*, **332**, 958, 1998A&A...332..958B

Burki, G. & Meylan, G., *Astronomy and Astrophysics*, **159**, 261, 1986A&A...159..261B

Carney, B. W. et al. 1994, *The Astronomical Journal* , **107**, 2240, 1994AJ....107.2240C

Carney, B. W. et al. 2001, *The Astronomical Journal* , **122**, 3419, 2001AJ....122.3419C

Ciucă, I. et al. 2021, *Monthly Notices of the Royal Astronomical Society* , **503**, 2814, 2021MNRAS.503.2814C

Coates, D. W., Halprin, L. & Thompson, K. 1982, *Monthly Notices of the Royal Astronomical Society*, **199**, 135, 1982MNRAS.199..135C

Cohen, R. E. & Sarajedini, A., *Monthly Notices of the Royal Astronomical Society*, **419**, 342, 2012MNRAS.419..342C

Eker, Z. et al. 2018, *Monthly Notices of the Royal Astronomical Society* , **479**, 5491, 2018MNRAS.479.5491E

Flower, P. J. 1996, *The Astrophysical Journal*, **3**, 469, 355, 1996ApJ...469..355F

Fu, J. N. et al. 2009, *Publications of the Astronomical Society of the Pacific*, **121**, 251, 2009PASP..121..251F

Gajdoš, P. & Parimucha, Š. 2023, *Open Europ. Journal on Var. Stars*, **241**

Green, G. M. 2018, *Journal of Open Source Software*, **3**, 26, 695, 2018JOSS....3..695G

Hintz, E. G. et al. 2004, *Publications of the Astronomical Society of the Pacific*, **116**, 543, 2004PASP..116..543H

Hübscher, J. et al. 2010, *Information Bulletin on Variable Stars*, **5941**, 2010IBVS.5941....1H

Hübscher, J. & Monninger G. 2011, *Information Bulletin on Variable Stars*, **5959**, 2011IBVS.5959....1H

Hübscher, J. 2011, *Information Bulletin on Variable Stars*, **5984**, 2011IBVS.5984....1H

Hübscher, J. 2015, *Information Bulletin on Variable Stars*, **6152**, 2015IBVS.6152....1H

Hübscher, J. 2016, *BAV Journal*, **2**, 2016BAVJ....2....1H

Kozar, T. 1980, *Information Bulletin on Variable Stars*, **1834**, 1980IBVS.1834....1K

Lenz, P. & Breger, M. 2005, *Communications in Asteroseismology*, **146**, 53, 2005CoAst.146...53L

Li, L. J. & Quian, S. B. 2010, *The Astronomical Journal*, **139**, 6, 2639, 2010AJ....139.2639L

Mahdy, H. A. & Szeidl, B. 1980, *Communications of the Konkoly Observatory*, **74**, VII.9.1, 1980CoKon..74....1M

Malkov, O. Yu. et al. 2012, *Astronomy and Astrophysics*, **546**, 69, 2012A&A...546A..69M

Masani, A. & Broglia, P. 1954, *Memorie della Società Astronomia Italiana*, **25**, 431, 1954MmSAI..25..431M

Morgenroth, O. 1934, *Astron. Nachr.*, **252**, 389, 1934AN....252..389M

Netzel, H. & Smolec, R. 2022, *Monthly Notices of the Royal Astronomical Society* , **515**, 4574, 2022MNRAS.515.4574N

Pagel, L. 2018, *Information Bulletin on Variable Stars*, **6244**, 2018IBVS.6244....1P

Pagel, L. 2019, *BAV Journal*, **31**, 2019BAVJ...31....1P

Pagel, L. 2021, *BAV Journal*, **52**, 2021BAVJ...52....1P

Pagel, L. 2022, *BAV Journal*, **60**, 2022BAVJ...60....1P

Pagel, L. 2023, *BAV Journal*, **76**, 2023BAVJ...76....1P

Petersen, J. O. & Christensen-Dalsgaard, J. 1999, *Astronomy and Astrophysics*, **352**, 547, 1999A&A...352..547P

Poretti, E. et al. 2005, *Astronomy and Astrophysics*, **440**, 1097, 2005A&A...440.1097P

Prša, A. et al. 2016, *The Astronomical Journal*, **152**, 41, 2016AJ....152...41P

Quigley, R. & Africano, J. 1979, *Publications of the Astronomical Society of the Pacific*, **91**, 230, 1979PASP...91..230Q

Salaris, A. et al. 1993, *The Astrophysical Journal*, **414**, 580, 1993ApJ...414..580S

Schlegel, D. J., Finkbeiner, D. P. & Davis, M. 1998, *The Astrophysical Journal*, **500**, 525, 1998ApJ...500..525S

Schneller, H. 1938, *Die Sterne*, **18**, 277

Soloviev, A. 1934, *Tadjik Observatory Circular*, **37**

Steinmetz, C. H. D. 1946, *Bulletin of the Astronomical Institutes of the Netherlands*, **10**, 178, 1946BAN....10..178S

Torres, G. 2010, *The Astronomical Journal*, **140**, 5, 1158, 2010AJ....140.1158T

Wehlau, R. & Leung, K.-C. 1964, *The Astrophysical Journal*, **139**, 843, 1964ApJ...139..843W

Vallenari, A. et al. (Gaia collaboration) 2023, *Astronomy and Astrophysics*, **674**, A1, Gaia collaboration

Wenger, M. et al. 2000, *Astronomy and Astrophysics Supplement*, **143**, 9, 2000A&AS..143....9W

Xue, H. F. & Niu, J. S. 2020, *The Astronophysical Journal*, **904**, 1, 2020ApJ...904....5X

https://oejv.physics.muni.cz
October 2024 DOI: 10.5817/OEJV2024-0254 ISSN 1801–5964

Appendix A

In order to analyze the behavior of the (O-C) values, the following new times of maximum light were used in addition to those mentioned in the studies of Hintz et al. (2004) and Xue & Niu (2020). To avoid the potential for statistical overestimation, only a representative subset of the data from the TESS satellite was utilized.

Sources:
(a) Pagel (2018); (b) Huebscher et al. (2010); (c) Huebscher & Monninger (2011), (d) Huebscher (2011), (e) Huebscher (2015); (f) Huebscher (2016); (g) Pagel (2019); (h) Pagel (2023); (i) Pagel (2022); (k) Pagel (2021); (m) AAVSO International Database; (n) TESS/Mikulski Archive for Space Telescopes (MAST); (o) BAV internal web archive; (p) this paper

October 2024 DOI: 10.5817/OEJV2024-0254 ISSN 1801–5964

Table 9: Times of maximum light

J.D. (hel.)	Error [d]	Source	J.D. (hel.)	Error [d]	Source	J.D. (hel.)	Error [d]	Source
2455062.5188	0.001	a	2459131.6491	0.0008	m	2459735.84032	0.0005	m
2455062.5916	0.001	a	2459131.7197	0.0005	m	2459796.73377	0.0005	m
2455068.4982	0.001	b	2459131.7936	0.0009	m	2459813.3602	0.008	h
2455091.398	0.0009	b	2459136.4609	0.0005	m	2459813.4329	0.007	h
2455091.4707	0.0007	b	2459136.5336	0.0008	m	2459816.4236	0.0035	h
2455091.5436	0.0007	b	2459136.6068	0.0009	m	2459820.4343	0.014	h
2455093.3656	0.0035	b	2459160.3078	0.0005	m	2459824.44509	0.0007	m
2455097.3769	0.0021	b	2459164.2457	0.0005	m	2459824.51835	0.0008	m
2455185.2524	0.0006	c	2459164.3181	0.0005	m	2459824.59086	0.0007	m
2455189.1908	0.0027	c	2459164.3913	0.0005	m	2459826.70680	0.0003	n
2455192.1799	0.0008	c	2459451.4288	0.0002	i	2459830.71695	0.0005	m
2455192.2538	0.0013	c	2459451.501	0.0004	i	2459830.7896	0.0006	m
2455378.5066	0.0021	c	2459422.4773	0.0003	i	2459830.86281	0.0005	m
2455439.4733	0.0035	d	2459422.551	0.0004	i	2459833.19740	0.0004	n
2455444.5053	0.0014	d	2459423.4993	0.001	i	2459842.45910	0.0003	n
2455446.4011	0.0028	d	2459423.5704	0.0007	i	2459845.3757	0.0021	h
2455451.5064	0.0028	d	2459425.541	0.0012	i	2459846.76152	0.0004	n
2455453.3285	0.0035	d	2459432.6163	0.0007	i	2459931.4278	0.035	o
2456200.384	0.0035	e	2459433.5636	0.001	i	2460170.4812	0.0006	o
2456928.4038	0.0056	e	2459461.4196	0.002	m	2460170.5534	0.0006	o
2456928.4039	0.0056	e	2459461.49145	0.0006	m	2460179.5232	0.0008	o
2456928.4043	0.0056	e	2459464.62862	0.0004	m	2460179.5961	0.0006	o
2456981.3496	0.0035	e	2459464.7013	0.0004	m	2460179.59487	0.0004	m
2456981.4225	0.0035	e	2459464.77383	0.0004	m	2460194.3997	0.0017	p
2457241.4047	0.0009	f	2459464.84667	0.0005	m	2460195.3481	0.0017	p
2457241.4759	0.0008	f	2459466.3789	0.017	i	2460214.30828	0.0005	m
2457242.498	0.0005	f	2459474.61922	0.0005	m	2460214.38112	0.0005	m
2457965.4159	0.0017	g	2459474.69253	0.0004	m	2460218.38947	0.0005	m
2457970.4464	0.001	g	2459474.76535	0.0004	m	2460218.46243	0.0007	m
2458388.3853	0.004	g	2459495.40194	0.0006	m	2460218.61049	0.0005	m
2458721.368	0.002	h	2459496.3512	0.0035	i	2460218.68389	0.0004	m
2458721.3695	0.001	i	2459497.2993	0.017	i	2460218.75617	0.0004	m
2458721.441	0.001	h	2459497.3733	0.035	i	2460220.58007	0.0004	m
2458721.4411	0.009	i	2459510.49865	0.0006	m	2460220.65077	0.0004	m
2459111.375	0.0001	k	2459510.57286	0.0008	m	2460220.7256	0.0004	m
2459112.6144	0.0004	m	2459536.24127	0.0005	m	2460225.32234	0.0008	m
2459112.6864	0.0004	m	2459536.31437	0.0008	m	2460225.39308	0.0007	m
2459112.7603	0.0006	m	2459541.27293	0.0004	m	2460262.29241	0.0004	m
2459112.8333	0.0009	m	2459541.34643	0.0005	m	2460262.36429	0.0003	m
2459131.5752	0.0005	m	2459559.28589	0.0005	m			